Journal of Marine Science and Engineering

MDPI

Article

The Environmental Assessment of an Estuarine Transitional Environment, Southern Italy

Michele Arienzo [1,*], Francesco Bolinesi [2], Giuseppe Aiello [1], Diana Barra [1], Carlo Donadio [1], Corrado Stanislao [3], Luciano Ferrara [4], Olga Mangoni [2], Maria Toscanesi [3], Antonella Giarra [3] and Marco Trifuoggi [3]

[1] Department of Earth Sciences, Environment and Resources, University of Naples Federico II, Via Vicinale Cupa Cintia 21, 80126 Naples, Italy; giuseppe.aiello@unina.it (G.A.); diana.barra@unina.it (D.B.); carlo.donadio@unina.it (C.D.)

[2] Department of Biology, University of Naples Federico II, Via Vicinale Cupa Cintia 21, 80126 Naples, Italy; francesco.bolinesi@unina.it (F.B.); olga.mangoni@unina.it (O.M.)

[3] National Fire Corps, Department of Firefighters, Public Rescue and Civil Defense, Strada Val Nure 9, 29122 Piacenza, Italy; corrado.stanislao@gmail.com (C.S.); maria.toscanesi@unina.it (M.T.); antonella.giarra@unina.it (A.G.); marco.trifuoggi@unina.it (M.T.)

[4] Department of Chemical Sciences, University of Naples Federico II, Via Vicinale Cupa Cintia 21, 80126 Naples, Italy; luciano.ferrara@unina.it

* Correspondence: michele.arienzo@unina.it

Received: 10 July 2020; Accepted: 17 August 2020; Published: 19 August 2020

Abstract: A multidisciplinary survey was carried out on the quality of water and sediments of the estuary of the Sele river, an important tributary of the Tyrrhenian Sea, to assess anthropogenic pressures and natural variability. Nine sediment sites were monitored and analyzed for granulometry, morphoscopy, benthic foraminifera and ostracod assemblages, heavy metals, and polycyclic aromatic hydrocarbons. Surface water was assayed for ionic composition and phytoplankton biomass. Total organic carbon (TOC) and total nitrogen (TN) in sediments were higher in the inner part of the estuary (IE), up to 12.7 and 0.7% because of anthropic influence. In waters, $N\text{-}NH_4$, $N\text{-}NO_3$, and $P_{tot.}$ were high, with loads of P_{tot} in IE exceeding ~fourfold the limit. Here, it was also observed that the highest primary production was Chl-a, 95.70 μg/L, with cryptophytes, 37.6%, and diatoms, 33.8%, being the main phytoplanktonic groups. The hierarchical analysis split the estuary into two areas, with marked differences in anthropic pollution. Waters were classified as poor–bad level with respect to the content of nutrients. Sedimentological assay reveals littoral erosion and poor supply of river sandy sediments. The erosion environment is confirmed by the presence of meiobenthic recent marine forms intrusion inside the river. All these data reveal the fragility of the estuary and the need of urgent remediation actions.

Keywords: marine transitional environment; estuary; sedimentology; water-sediment quality; foraminifers and ostracods; eutrophication

1. Introduction

Estuary areas are those in which the waters of the rivers that join the sea are influenced by the tides, with progressive mixing and presence of salinity and density gradients. The difference in density between fresh and marine waters by gravity produces a vertical stratification of salinity and a convective flow (estuarine circulation) [1]. The variability of the physical–chemical, climatic and morphological parameters between environments belonging to the same typology, however, is such that each area constitutes a separate environment with peculiar characteristics that are difficult to

generalize and classify. [2]. These environments are complex systems to be analyzed since numerous factors contribute to their variability. The morphology of each area is influenced by annual, seasonal, and even daily variations, both climatic (humidity, rain, temperature, winds) and physicochemical (salinity, oxygen, ionic composition) [3]. These elements, in turn, influence each other, defining particular conditions of spatial and temporal heterogeneity in the same areas; thus numerous gradients are created, such as that of salinity with greater salinity towards the sea and less rising towards the interior of the river; the variation is then more or less accentuated according to the morphology of the watercourse and the presence or absence of tributaries [3–6].

In transitional areas, water quality could be adversely affected by anthropogenic activities, such as the application of agricultural fertilizers and manure, and the discharge of wastewater from urban and industrial sources [7].

Due to the great variability and presence of different gradients, the transition waters environments are very fragile and easily subject to dystrophic crises. Another issue is erosion caused by seawater intrusions and river flow, causing degradation of water quality and aquatic habitat. Excessive amounts of sediment, resulting from natural or human-induced causes, can result in the reduction of diversity and abundance of aquatic life. If the river cross-section is sufficiently reduced by a sediment build-up, sedimentation can increase downstream flooding. Also, some trace elements, (TEs), ions, pesticides, and nutrients may adhere to sediment particles and be transported downstream [8].

The Sele River is an important watercourse in Campania, 64 km long, the second in the region after the Volturno River, and a tributary of the Tyrrhenian Sea [9]. The river, located within an alluvial plain, has a drainage basin of 3235 km^2 and a solid flow of 500,000 m^3/yr [10], embedded in the natural reserve of Foce Sele-Tanagro (Figure 1). However, the presence of the Dam of Persano, 16.2 linear km from the river mouth, built between 1929 and 1932 and creating a basin of 1.5 million m^3, affects the downstream sediment deposition causing the consequent retreat of the coast [11–13]. This, together with sediment removal from the dune ridge and the beaches and the anthropogenic pressure along the littoral, locally contributes to erosion. The literature lacks data on the environmental status of the Sele estuary (SE). The current study tries to fill this gap through a multidisciplinary approach determining the sedimentological, chemical, and meiobenthic features of the superficial sediments as well as the water quality of the SE. It was also evaluated if the SE and the surrounding beach is retreating because of anthropic activities.

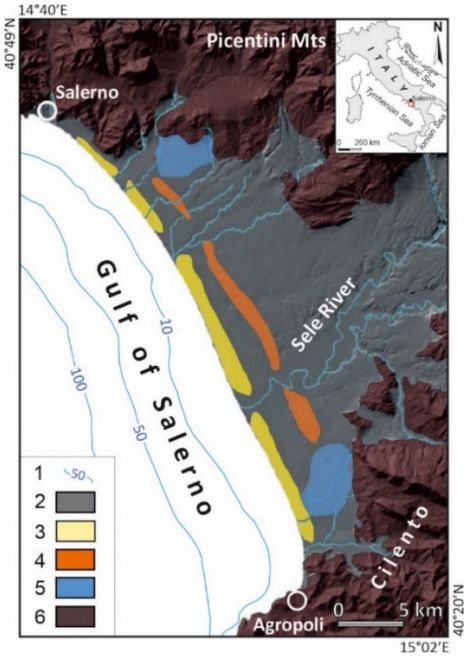

Figure 1. Geological map of the Sele River plain: 1) isobath (meters below sea level); 2) alluvial, transition and marine deposits (Quaternary); 3) coastal dune sandy deposits (Holocene); 4)

palaeodune sandy deposits of Gromola-Santa Cecilia-Arenosola-Aversana (Late Pleistocene); 5) travertine deposits (Middle Pleistocene-Holocene); 6) carbonate (Picentini Mts) and terrigenous (Cilento Promontory) formations (Meso-Cenozoic). The geographic coordinate system is WGS84.

2. Materials and Methods

The Sele River plain extends along the middle sector of Salerno province territory. The plain has a triangular surface area of about 400 km^2. It is bounded seaward by a narrow sandy coastal strip, between the towns of Salerno (NW) and Agropoli (SE), and landward it is bordered to the north and northwest by the Lattari and Picentini Mountains and to the southeast by the Alburni Mountains and Cilento Promontory (Figure 1). At the base of the Eboli hills, a terraced surface, ranging between 100 and 30 m above sea level, is formed by the Middle Pleistocene Persano Formation [14,15] mainly constituted by alluvial, fluvial-marshy, lagoon, and marine deposits. Further seaward, the coastal plain is characterized by the presence of three orders of beach-dune ridges formed during the last interglacial, which interfinger to the rear with lagoon and fluvial-palustrine deposits. The Sele River alluvial-coastal plain was affected by the same morpho-sedimentary behavior, with a transgressive trend during the early Holocene and a retreating trend of shorelines starting from middle Holocene [15–19]. The plain is characterized by high agricultural productivity, and livestock farming (buffalo farms) are very well developed. The provincial horticultural production covers a wide range of vegetables and fruits, which generally feeds the local food industry [20]. The industrial activities are numerous and include, apart from canneries, numerous dairies, and chemical industries. Furthermore, there are several potentially contaminated sites (PCS) (both authorized landfills and unauthorized waste disposal areas), localized across the territory by the regional environmental agency [21]. In areas where the main industrial activities are the processing of agricultural and livestock products, the emissions of wastes with a high load of organics and inorganics may affect environmental and ecological integrity.

A total of nine sites in three replicates per site were sampled by a Van Veen grab in July 2017: S1, S2, S3, S4, and S5 in the outer estuary (OE), and S6, S7, S8 and S9 in the inner estuary (IE) at a distance from 379 to 3245 m from OE, Figure 2. Granulometry and morphoscopic characteristics of the surfaces of quartz granules were determined [22,23]. After washing and oven drying at 80 °C for 72 h, mechanically quartered, samples were weighed with an analytical balance and sieved by a series of stacked sieves up to 63 μm with 1/2 ϕ class interval, in a mechanical sieve shaker for 15′. Fractions from 63 to 2 μm were analyzed through sedimentation in distilled water with 10% sodium oxalate at specific temperatures, [24]. The granulometric fraction percentages, sediment classification, and statistical parameters, according to the graphic method of [25] are shown in Table 1.

For each sample histograms and cumulative curves were plotted [26] by Gradistat v.8 software, which gives mean size (Mz), mode (M_ϕ), standard deviation (σ, sorting), skewness (S_{KI}, asymmetry coefficient), and kurtosis (K_G, appointment coefficient), as shown in Table 1. Samples were also analyzed by an optical stereomicroscope Leica MZ16 equipped with the software TriPlot v.1.4 [27] to identify the shape of quartz granules embedded in the 384–177 μm range [22]. In the sand fraction of 250 μm, 100 granules of different shapes for each sample were counted. In total, 900 particles were classified as: (1) not abraded, but transparent and angular (NA); (2) blunt-edged translucent, with subrounded to rounded edges, more or less hyaline (BT), and (3) rounded opaque, with well-rounded edges and opaque (RO).

For the determination of benthic foraminifera and ostracod assemblages, 200 g of dried sediments were washed through 230 and 120 mesh sieves (63 μm and 125 μm, respectively) and split. Foraminifera and ostracod shells were picked up from the coarser fraction, classified, and counted for quantitative analysis. Ostracods were counted as the total number of valves (TNV; the number of all the valves, including juveniles).

Table 1. Localization of sampling stations, particle size distribution, total organic carbon (TOC), and total nitrogen (TN), Carbon/Nitrogen ratio (C/N), granulometric classification, mean size (Mz), standard deviation, σ, skewness, Sk_I, kurtosis, K_G, and morphoscopic analysis of sediments.

Sample	Latitude N	Longitude E	* D	Depth	TOC	TN	C/N	Gravel	Sand	Silt	** Classification	Mz	σ	Sk_I	K_G	Morphoscopy (%)		
			m	m	%	%		%	%	%		*** ϕ	ϕ	ϕ	ϕ	NA	BT	RO
S1	40°29′05.05″	14°56′25.54″	350	1.0	0.4	<0.1		0.1	99.9		medium sand	1.62	0.561	−0.092	1.01	68	22	10
S2	40°28′55.32″	14°56′32.17″	39	1.0	1.0	<0.1			99.9	0.1	medium sand	1.64	0.617	0.010	0.952	68	30	2
S3	40°28′53.41″	14°56′34.81″	85	1.5	2.2	<0.1		74.0	26.0		very fine gravel	−1.93	1.267	0.307	0.825	89	10	1
S4	40°28′56.03″	14°56′35.82″	116	1.0	1.5	<0.1		30.3	69.7		very coarse sand	−0.56	1.830	−0.494	0.656	68	25	7
S5	40°28′55.49″	14°56′36.92″	144	1.5	2.4	0.2	12.00	7.4	68.5	24.1	fine sand	2.94	2.129	−0.376	1.92	76	21	3
S6	40°28′55.29″	14°56′46.83″	379	1.5	1.7	0.2	8.50	0.7	91.9	7.4	very fine gravel	3.46	0.581	−0.185	1.49	88	11	1
S7	40°28′55.28″	14°57′26.53″	1310	2.0	1.9	0.2	9.50	3.3	50.5	46.2	very fine sand	3.85	1.927	−0.127	1.46	75	20	5
S8	40°29′28.24″	14°58′12.27″	2586	2.0	1.6	0.2	8.00	14.9	81.0	4.1	coarse sand	0.66	1.580	−0.311	2.09	69	23	8
S9	40°30′01.78″	14°58′18.37″	3246	2.0	12.7	0.7	18.14	7.4	69.9	22.7	fine sand	2.34	2.015	−0.049	0.875	94	5	1

* Distance from the river mouth, ** according to Folk and Ward (1957), *** $\phi = -\log_2 Ø_{mm}$, NA not abraded; BT, blunt-edged transparent; RO, rounded opaque granule.

Figure 2. Sampling points are indicated in red circles (after Google Earth™ Pro, 2019).

The determination of TOC/TN was performed by an elemental analyzer Primacs$^{SNC-100}$ Skalar (Breda, The Netherlands); 0.5 g of ≤2000 μm dry sediments were weighed in ceramic vessels and combusted at high-temperature range 900–1100 °C chamber in the presence of oxygen. The gases of carbon dioxide and nitrogen were separated and measured with a non-dispersive infrared detector (NDIR) e thermal conductivity detector (TCD). Total organic carbon was determined by the difference of total carbon (TC) and inorganic carbon (IC) concentration. TC was determined by catalytic oxidation of the sample at 1100 °C, converting the carbon to CO_2, which was detected by the NDIR detector. IC was determined by acidification of the sample with phosphoric acid solution (20% v/v), which converts the IC to CO2, which was detected by the NDIR detector.

The ≤2000 μm fraction was used for the analyses of the total pool of Al, As, B, Ba, Be, Cd, Co, Cr, Cu, Hg, Mn, Ni, Pb, Sb, Se, V, and Zn by digesting about 0.5 g of sediment in 12 mL of H_2O_2-HNO_3, in Teflon vessels in an Ethos Plus microwave lab station (Milestone) for 15 min; the obtained solution was taken to a final volume of 100 mL with 5% HCl and then filtered by 0.45 μm [28].

Chemical characterization of the elements was performed by ICP-AES by a Thermo Electron Corporation IRIS Intrepid II spectrometer. Sixteen PAHs indicated from Environmental Protection Agency (EPA) as important toxicological contaminants were determined: acenaphthene (ACE), acenaphthylene (ACY), anthracene (ANT), benzo(a)anthracene (BaA), benzo(b)fluoranthene (BbF), benzo(k)fluoranthene (BkF), benzo(ghi)perylene (BgP), benzo(a)pyrene (BaP), chrysene (CHR), dibenz(ah)anthracene (DhA), fluoranthene (FLT), fluorine (FLR), indene (IND), naphthalene (NAP), phenanthrene (PHE), and pyrene (PYR). Among these NAP, ANT, BbF, BkF, BaP, and BgP represent the priority dangerous PAHs, and their sum is regulated by the law. For the analysis of PAHs, the IRSA CNR 25 method was followed and modified by replacing cyclohexane with acetone/n-hexane 1:1 v/v and using a longer sonication time of 3 h by an ultrasonic disruptor, Branson (US), with a power of 300 W in pulsed mode. Details of the adopted method are given in [29]. Mean recoveries ranged from a minimum of 85% to a maximum of 97%. Stations S5, S6, S7, S8, and S9 were also monitored for the quality of water. Surface water was collected at 0.25 m below the surface in a vial of 20 mL from the Niskin bottle and stored at 4 °C until they were analyzed. NO_2, NO_3, and NH_4 were analyzed following the procedure described by Hansen and Grasshoff [30], whereas PO_4, NH_4, NO_3, and NO_2 were determined by that outlined by Baird et al. (2017). Samples were also analyzed for pH (APAT CNR IRSA, 2003), temperature (°C), electrical conductivity (EC, dS/m) (APAT CNR IRSA, 2003). Cations, Ca, Mg, Na, K, and anions, Cl, F, SO_4 were determined by ionic chromatography and conductimetric detector [31]. Al, As, Ba, Be, Cd, Co, Cr, Cu, Fe, Hg, Mn, and Ni were determined by acid digestion and ICP-MS [32].

To assess the phytoplankton biomass and diversity, in terms of larger taxonomical groups, surface water samples were collected with a Niskin bottle. One liter of water was then drawn from the Niskin and filtered on GF/F Whatman filters (47 mm and 25 mm diameters). Filters were stored at −20 °C until spectrofluorimetric and HPLC analyses for pigment spectra determinations [33,34]. The amount of Chl-a was used to indicate the total phytoplankton biomass, whereas phaeopigments, i.e., the main Chl-a degradation products, are indicators of grazing activity [35] and estimate the senescence of phytoplankton populations [36,37]. The contribution of the main phytoplankton groups to the total Chl-a was estimated on the basis of the concentrations of biomarker pigments, using the chemical taxonomy software CHEMTAX [38,39].

Statistical analysis consisted of a Pearson's correlation matrix, a principal component analysis (PCA), and hierarchical cluster analysis (HCA) and was performed by STATISTICA v.5 (StatSoft Inc., Tulsa, OK, USA).

3. Results and Discussion

3.1. Sedimentology

Table 1 indicates that water was very shallow, with an average depth of 1.50 m and became deeper, up to 2.00 m, at S7, S8, and S9. Granulometry varies from medium sand, $1.62 < Mz < 2.94$ ϕ, in the OE, S1–S5, to fine or very fine sand class in IE, $2.34 < Mz < 3.85$ ϕ. The sand ranges between 50.5

and 99.9%, with the exception of S3, 26%. The silt is mainly absent along the estuary and varies from 4.1 to 46.2% in the inner sector, S5–S9, and no clay was detected. Sediments can be classified as very fine sand—very fine gravel, with a prevalence of finer grains in the IE. Most of the samples are bimodal and multi-modal, S3, S4, S5, S7, S8, and S9, which is composed of two or more mixed granulometric classes. Figure 3a reports the granulometric spindle grouping the cumulative curves and reveals that samples mostly fall in the dimension range from –2 to 4 ϕ. The data of Table 1 and Figure 3a highlights that the river can transport and deposit materials of different granulometry almost at the same time and leave gravel or sand with varying speed and hydrodynamic energy. Thus, at any point, the sand can infiltrate between the gravel previously deposited, or the pebbles sporadically reach a predominantly sandy deposit. The sorting coefficient σ is low, ~0.6 ϕ, i.e., sediments have a high grade of selection, for a few samples located mostly close to OE, S1, S2, and S6. The remainder samples, $\sigma > 1.2$ ϕ, have rather low selection grade indicating a high energy and erosion environment. Another important parameter which explains the hydrodynamic energy is the asymmetry S_{KI}. Most of the values, Table 1, are negatives, $-0.05 > S_{KI} > -0.49$ ϕ, indicating a prevalence of coarse sediments related to the modal class, and a high-energy environment. This means both erosion and lack of accumulation of fine sediments from the river, causing beach retreat. The coefficient of appointment K_G is high for some inner mouth samples, S5, S6, S7, and S8, $1.46 < K_G < 2.09$ ϕ, and low or medium for the remaining ones, $0.66 < K_G < 1.01$ ϕ indicating a uniformity in the distribution of granulometric fractions. Thus, the data reveal that the estuary represents an environment affected by littoral erosion and with a poor supply of river sandy sediments.

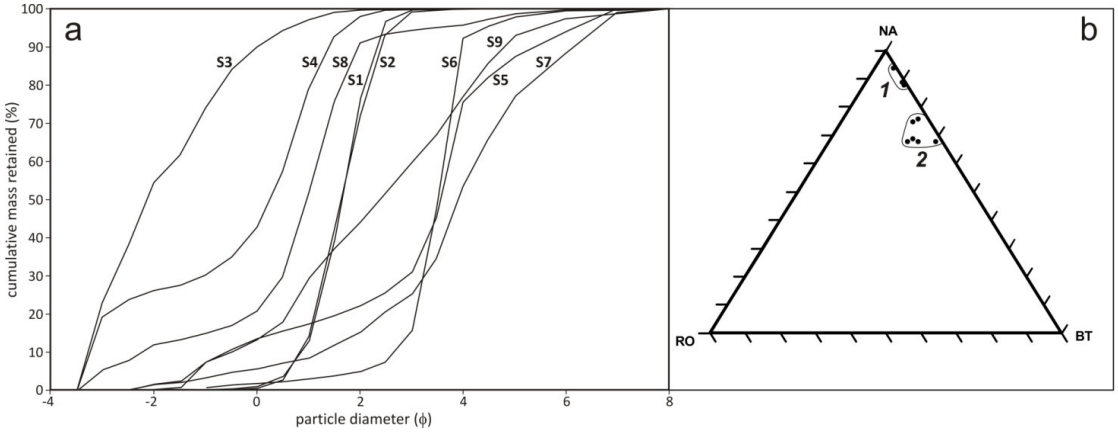

Figure 3. Granulometric spindle grouping the cumulative curves (**a**) and ternary diagrams of quartz granules morphoscopy (**b**) of the 9 sediment samples (S1–S9): NA, transparent not abraded; BT, blunt-edged; RO, rounded opaque; 1, fluvial-marine and 2, actual and paleodune granules group.

Figure 3b shows the morphoscopy ternary diagram based on the analysis of quartz granules. Two groups were identified: group 1, S1–S4, with transparent granules not abraded and angular (NA, 77%) or slightly blunt-edged (BT, 19%); group 2, S1, S4, S7, and S8, with some well-rounded opaque granules (RO; 4%). These data reveal a short transport along the estuary and the beach impeding high rounding of particles, group 1. The rounded grains along the riverbed are attributable both to the actual dune and Pleistocene paleodune of Gromola downstream S9, group 2, eroded by the river and its tributaries. Generally, the low number of quartz granules confirms that the river erodes mainly carbonate lithologies. In this transition environment, the sand from different sources can infiltrate between the gravel previously deposited, or the pebbles sporadically reach predominantly sandy sediment.

3.2. Meiobenthos Features

Table 2 reports the planktonic and benthic foraminiferal and ostracod assemblages. A total of 150 foraminiferal tests and 22 ostracod valves were recorded. All the planktonic foraminiferas, 105

tests, and part of benthic foraminiferas are regarded as allochthonous, belonging to the upper Quaternary sediments of the Gromola Synthem geological formation [40] and transported by the river. Planktonic foraminifers tended to shift from common in S5 to uncommon or rare in IE, which was interpreted as reflecting inputs of marine waters into the river [41]. The benthic foraminiferal assemblages consisted of 13 species assigned to 11 genera. Foraminifera were widely distributed in sand flats, mudflats, and marshes at the mouths of the estuaries and represented a mean to study palaeo-macro-tidal estuarine environments and the extent of sea-level change in estuarine settings [42]. Two main genera of intertidal foraminifers were identified: Ammonia, making up ~33%, and Cibicidoides, ~31%, characteristic of a low marsh at the mouths of the estuaries [42]. A slight difference in spatial distribution was observed between the two groups with a higher presence of Ammonia towards OE and of Cibicidoides in IE. The presence of all other species is discontinuous and rarely exceeds 6%.

Table 2. Quantitative (individuals/100 g of dried sediment) distribution of benthic foraminifer and ostracod (MNI = Minimum Number of Individuals; TNV = total number of valves) assemblages, and semi-quantitative distribution of the remaining taxa (a = abundant, c = common, u = uncommon, r = rare, vr = very rare).

Samples	S3	S5	S6	S7	S8	S9
Foraminifera (planktonic)		C		R	U	U
Foraminifera (benthic)						
Ammonia aberdoveyensis Haynes, 1973 lobate form		7	6			
Ammonia aberdoveyensis Haynes, 1973 rounded form			1		1	
Brizalina spathulata (Williamson, 1858)					1	1
Cassidulina carinata Silvestri, 1896					1	
Cibicidoides sp.		3		3	2	6
Discorbidae				1		
Elphidium poeyanum (d'Orbigny, 1839)		1				
Elphidium punctatum (Terquem, 1878)					1	
Haynesina germanica (Ehrenberg, 1840)					1	
Melonis sp.		3				
Planulina ariminensis d'Orbigny, 1826		1				
Planulina sp.				1		
Triloculina trigonula (Lamarck, 1804)			1			
Uvigerina mediterranea Hofker, 1932					2	1
Ostracoda						
Aurila sp.			5			
Candona neglecta Sars, 1887			2			
Cryptocandona sp.			1			
Ilyocypris bradyi Sars, 1890			2			
Mixtacandona laisi (Klie, 1938)			2			
Pontocythere turbida (Müller, 1894)			1			
Prionocypris zenkeri (Chyzer and Toth, 1858)			2			
Pseudocandona sarsi (Hartwig, 1899)			6			
Semicytherura sulcata (Müller, 1894)	1					

Ostracod assemblages, Table 2, were detected only in S6, with the exception of S3, where only one ostracod specimen was found and included nine species belonging to nine genera. Two species, *Aurila* sp. and *Cryptocandona* sp., represented only by very young instars, have been left in open nomenclature. The dominant species were *Pseudocandona sarsi* and *Aurila sp.* making up 27 and 23% of total presences. Three species of genera, *Aurila*, *Pontocythere*, and *Semicytherura*, are typical of the shallow marine environment, and six, *Candona neglecta*, *Cryptocandona* sp., *Ilyocypris bradyi*, *Mixtacandona laisi*, *Prionocypris zenkeri*, *Pseudocamdona sarsi*, of continental waters [43]. Data revealed the constant presence of allochthonous circalittoral marine forms presumably from erosion of the Pleistocene sandy paleodune ridge of Gromola, cut by the river and some tributaries further east paleodune. The detection of the presence of recent marine forms up to S8 in IE is an indication of

progressive seawater intrusion. This represents the maximum intrusion limit of the seawater inside the river, of about 2600 m.

3.3. Sediment Chemical Data

Sediment chemical data are reported in Table 1. The mean amount of TOC in OE was 1.5%, with a minimum of 0.4% at S1. In IE, TOC values were higher, 4.5%, with a maximum of 12.7% at S9. This was expected since S9 station is facing a channel carrying industrial wastewater. In parallel, TN content was <0.1% in OE and increased in IE up to 0.7% at S9, indicating a marked anthropic influence. The IE is, in fact, affected by wastewater discharges by the entry of numerous canals. TOC and TN represent important parameters for the estimation of the environmental status of SE. The sediment organic carbon and nitrogen may derive by decomposition of plants or plankton or anthropogenic sources [44]. Regardless of the source, the portion of TOC and TN affect the faunal communities [45,46], the primary production, and the eutrophication status [47]. As shown in Table 1, there is a certain tendency for TOC and TN concentrations to decrease seaward, from 12.7 and 0.7% in IE to 0.4 and <0.1% in OE. This implies that anthropogenic input influences the accumulation of organic matter in IE surface sediments. The spatial difference of TOC among IE sediments is significant due to multiple immission of wastewater discharging canals. The C/N elemental ratio is an indicator of the predominant sources of organic matter in aquatic ecosystems [48,49]. The C/N ratios of undegraded marine phytoplankton are generally close to 6.7, while vascular plants are N-depleted and have ratios >12 [49]. Anthropogenic activities may alter the C/N ratios of organic matter from natural origins. Table 1 shows C/N ratios for the IE ranging from 8.00 to 18.14, indicating that the terrestrial materials from the river and the anthropogenic influence could be an important source of organic matter in sediments. It was also found an exceptionally high R^2, ~1.0, between C/N and TOC revealing a significant disturbance from the anthropogenic pressure.

The concentration of total priority dangerous PAHs in sediments was <0.01 mg/kg (data not shown) at all sites, and hence below the legal limit of 0.20 mg/kg expressed by the law 152/2006. Table 3 reports the concentrations of TEs in sediments, mg/kg. The levels of elements are below the legal limit, see Table 3, for As, Cd, Cr, Hg, Ni, and Pb at all sites. However, the mean concentration of Ni at S5, S6, and S7 were slightly lower the limit, ~22 vs. 30 mg/kg. TEs were of the same order of magnitude in S2, S3, S4, highlighting the greater influence of marine intrusion. They are, in fact, also comparable with those of S1 of known sea sources. TEs levels shifted towards higher levels in S5, S6, S7, S8, and S9, due to the greater influence of river flooding.

Table 3. Concentrations of elements in sediments of the Sele River estuary (mg/kg). Data were compared with those of the law 152/06 [50].

TEs	S1	S2	S3	S4	S5	S6	S7	S8	S9	Law limit 152/06 [50]
Al	4.83X10^3	4.19X10^3	5.70X10^3	4.35X10^3	27.5X10^3	22.8X10^3	25.8X10^3	27.0X10^3	20.6X10^3	
As	3.00	2.00	2.00	3.00	2.00	3.00	3.00	3.00	2.00	12.0
B	11.0	<1.0	<1.0	<1.0	15.0	22.0	32.0	25.0	33.0	
Ba	14.0	12.0	11.0	18.0	109	53.0	69.0	111	64.0	
Be	<0.50	<0.50	<0.50	<0.50	1.40	1.40	1.40	1.60	1.30	
Cd	<0.05	<0.05	<0.05	<0.05	<0.05	<0.05	<0.05	<0.05	<0.05	0.30
Co	4.00	4.00	4.00	4.00	8.00	8.00	7.00	6.00	5.00	
Cr	6.00	5.00	5.00	5.00	22.0	23.0	24.0	22.0	19.0	50.0
Cu	4.00	3.00	4.00	5.00	23.0	24.0	21.0	24.0	28.0	
Hg	<0.05	<0.05	<0.05	<0.05	0.06	0.08	<0.05	0.07	0.06	0.30
Mn	572	660	579	428	379	375	390	358	182	
Ni	13.0	13.0	13.0	13.0	21.0	22.0	21.0	16.0	14.0	30.0
Pb	3.00	3.00	2.00	2.00	15.0	14.0	12.0	18.0	10.0	30.0
Sb	<0.2	<0.2	<0.20	<0.20	<0.20	0.30	0.28	0.58	<0.20	
Se	<0.10	<0.10	<0.10	<0.10	<0.10	1.30	<0.10	<0.10	<0.10	
V	11.0	10.0	9.0	10.0	29.0	27.0	29.0	37.0	27.0	
Zn	18.0	14.0	17.0	18.0	55.0	61.0	57.0	70.0	93.0	

Table 4 reports the output of the Pearson correlation matrix (CM). A significant, p <0.05, a positive correlation was found between B, Ba, Be, Co, Cr, Cu, Hg, Ni, V, and Zn with an r range of 0.70–0.99, highlighting a common source. Only As and Se did not show any significant correlation, due to different provenience of the elements. A separate behavior seems to manifest Sb, which appeared significantly correlated only with Pb, r = 0.73, p <0.05, due to the well-known association of Sb with Pb in the environment [51]. Notwithstanding the absence of clay in all samples, some TEs like Al, B, Cr, and Ni showed a significant and positive correlation with silt, 0.68< r <0.72, p <0.05. There was also a positive correlation, r = 0.68, between silt and Mz. This gives greater weight to the weathering source and confirms that TEs are controlled by grain size. Normally, TEs content in terrigenous sediments increases in the sand silt-clay series and rises when moving from shelf to pelagic areas [52]. OE sediments were characterized by coarse grain sediments, Table 1, and showed lower TEs values, meaning scarce potential of coarser sized fabric to immobilize TEs.

Differently, TEs increased in inner sediments, S7, S8, and S9, where a high percentage of fine fractions occurred, up to 46.2% in S7, Table 1. There was a significant correlation, r = 0.92, p <0.001, between TOC and TN, indicating that nitrogen was mostly present in organic compounds [53]. Pearson coefficients seem to agree with the results from the principal component analysis, PCA. The loading factors, total and cumulative variance generated by PCA of TEs, TOC, silt, Mz, are shown in Table 5. Three principal components account for 82.8% of the total cumulative variance. PC1 explains 60.9% of the total variance and is significantly correlated with TN, Al, B, Ba, Be, Co, Cr, Cu, Hg, Ni, Pb, V and Zn, high positive load. PC2 explains 14.2% of the total variance and is very strongly and negatively correlated with TOC. PC3 explains 7.7% of the total variance and is slightly correlate with silt, positive load. These results, together with those from the Pearson's CM, show an evident association of most metals revealing a common source from terrestrial debris and anthropogenic sources. Furthermore, the higher presence of TEs in IE, Table 3, gives heavier weight to the anthropic enrichment. The results of the hierarchical cluster analysis, HCA, Figure 4, was performed by the criteria of Ward [54]. The diagram shows two main clusters, (A and B), very distinct at high hierarchical level, Figure. 4. This means that the studied sites split into two main groups which clearly characterize the estuary: cluster A, including sites S5–S9 in IE and cluster B, including sites S1–S4 in OE.

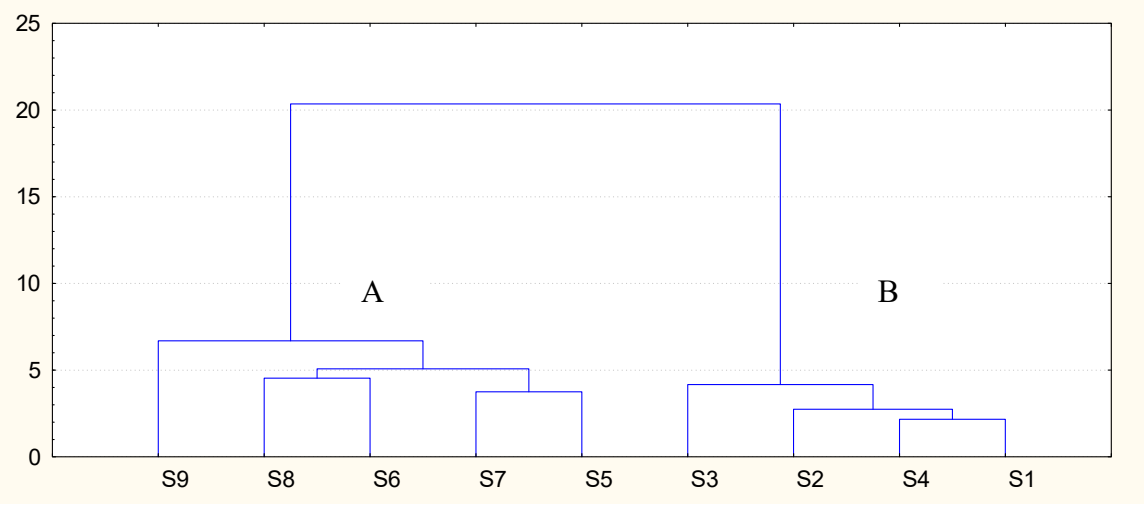

Figure 4. The output of hierarchical cluster analysis (HCA). Letters indicate clusters.

Table 4. Correlation coefficients among total organic carbon (TOC), total nitrogen (TN), sand, silt, mean size (Mz), and trace elements, TEs. In bold the values statistically significant (p <0.05). In bold = the high positive or negative loads.

	TOC	**TN**	**Sand**	**Silt**	**Mz**	**Al**	**As**	**B**	**Ba**	**Be**	**Co**	**Cr**	**Cu**	**Hg**	**Mn**	**Ni**	**Pb**	**Sb**	**Se**	**V**	**Zn**
TOC	1.00																				
TN	**0.92**	1.00																			
Sand	−0.17	−0.05	1.00																		
Silt	0.33	0.51	−0.34	1.00																	
Mz	0.15	0.44	0.39	0.68	1.00																
Al	0.25	0.59	−0.08	0.68	0.64	1.00															
As	−0.44	−0.25	0.27	−0.01	0.15	0.12	1.00														
B	0.51	**0.78**	0.01	**0.72**	0.68	**0.83**	0.23	1.00													
Ba	0.20	0.50	−0.03	0.53	0.47	**0.94**	0.05	0.69	1.00												
Be	0.33	0.66	−0.02	0.64	0.65	**0.99**	0.14	**0.87**	**0.91**	1.00											
Co	−0.03	0.31	0.01	0.59	**0.72**	**0.88**	0.17	0.60	**0.75**	**0.85**	1.00										
Cr	0.26	0.61	−0.03	**0.70**	**0.72**	**0.99**	0.19	**0.87**	**0.87**	**0.99**	**0.89**	1.00									
Cu	0.52	**0.80**	−0.02	0.62	0.63	**0.94**	0.05	**0.89**	**0.85**	**0.97**	**0.77**	**0.95**	1.00								
Hg	0.36	0.60	0.23	0.12	0.40	**0.75**	0.00	0.58	**0.74**	**0.80**	0.68	**0.74**	**0.84**	1.00							
Mn	**−0.71**	**−0.87**	0.12	−0.53	−0.40	**−0.73**	−0.09	**−0.80**	−0.67	**−0.78**	−0.50	**−0.74**	**−0.88**	−0.69	1.00						
Ni	−0.12	0.21	−0.03	0.64	**0.74**	**0.80**	0.23	0.56	0.64	**0.76**	**0.98**	**0.84**	0.68	0.53	−0.40	1.00					
Pb	0.14	0.50	0.08	0.49	0.58	**0.97**	0.19	**0.76**	**0.94**	**0.97**	**0.85**	**0.95**	**0.90**	**0.83**	−0.66	**0.75**	1.00				
Sb	−0.21	0.10	0.10	0.15	0.22	0.63	0.58	0.54	0.59	0.65	0.48	0.63	0.52	0.49	−0.31	0.44	**0.73**	1.00			
Se	−0.11	0.06	0.29	−0.10	0.38	0.24	0.32	0.19	0.02	0.30	0.53	0.35	0.31	0.52	−0.16	0.55	0.31	0.30	1.00		
V	0.27	0.61	0.02	0.58	0.57	**0.97**	0.20	**0.85**	**0.94**	**0.98**	**0.78**	**0.96**	**0.94**	**0.78**	**−0.75**	0.69	**0.98**	**0.73**	0.21	1.00	
Zn	0.68	**0.90**	−0.02	0.57	0.54	**0.85**	0.00	**0.91**	**0.77**	**0.91**	0.60	**0.86**	**0.97**	**0.79**	**−0.92**	0.49	**0.81**	0.47	0.21	**0.88**	1.00

Table 5. Loading factors, total and cumulative variance of total organic carbon (TOC), total nitrogen (TN), sand, silt, mean size (Mz), and trace elements (TEs). In bold = the high positive loads. PC1 and PC2 and PC3 are the abbreviations for principal components for the first factor, second, and third factor.

	PC1	PC2	PC3
TOC	0.381	**−0.873**	0.253
TN	**0.704**	−0.652	0.236
Sand	0.011	0.375	0.681
Silt	0.660	−0.205	−0.602
MZ	0.690	0.179	−0.035
Al	**0.976**	0.069	−0.158
As	0.147	0.647	0.118
B	**0.896**	−0.161	0.010
Ba	**0.879**	0.031	−0.135
Be	**0.994**	0.035	−0.035
Co	**0.843**	0.359	−0.187
Cr	**0.988**	0.106	−0.107
Cu	**0.985**	−0.141	0.079
Hg	**0.800**	0.030	0.460
Mn	**−0.817**	0.395	−0.158
Ni	**0.764**	0.430	−0.292
Pb	**0.944**	0.204	0.006
Sb	0.598	0.490	0.086
Se	0.330	0.498	0.443
V	**0.966**	0.067	−0.018
Zn	**0.926**	−0.318	0.172
Initial eigenvalue	12.786	2.991	1.614
% total variance	60.888	14.244	7.685
% cumulative variance	60.888	75.132	82.817

3.4. Water Quality Data

Chemical data are shown in Table 6. The average pH of the water was 7.9, with small differences among sites. Only at S9, was the pH significantly lower, (pH 7.3), indicating acid input. S9 as well as S8 were placed very close to the entry of canals releasing wastes from the many buffalo farms and runoff waters from intensive-grown soils of the plain. EC revealed to be quite similar in IE and OE, mean of 0.133 S/m, with low standard deviation, 0.027, indicating a scant influence of marine intrusion. Only in S7 EC was quite lower, 0.0842 S/m, due to a probable mixing with freshwaters. Cations were detected in the following order, Na > Ca > Mg > K, with mean values of 153.6, 99.0, 38.8, and 13.9 mg/L.

The range of variation of Ca and Mg between site S5, close to the estuary, and site S9, was very narrow, 99.7–107 and 40.2–44.2 mg/L. Na and K behaved differently, with higher Na values at the mouth, 199 vs. 150 mg/L, due to marine influence and higher K loads at S9, 23.9 vs. 12.6 mg/L. Na and K mean concentrations show more spatial fluctuation than Ca and Mg levels since both former cations are indicators of human activities [55]. It is interesting to note the progressive decrement of Na/Ca from the mouth to the inner portion of the river, from 2.00 to 1.42, due to the smoothing of marine intrusion. Concentrations of N-NH4 tended to significantly increase moving far away from the mouth, from 0.15 to 5.72 mg/L, with an increase of ammonium load of ~thirty folds. Regarding the presence of nutrients, the comparison with the benchmark regulatory values of the Ministerial decree 260/2010 and the Legislative Decree 152/06, allows for a partial classification of water concerning the content of $N\text{-}NH_4$, $N\text{-}NO_3$, P_{tot} within the class poor-bad level. At S9, nutrient pollution was extremely high, with loads of P_{tot} exceeding ~fourfold the limit of the worst quality class for P_{tot}.

The analyses of TEs found the sporadic presence of all the TEs listed above in concentrations below the fixed regulatory limit (SQA).

Table 6. Main chemical and physicochemical characteristics of the Sele River estuary at selected stations. Concentrations of cations and anions were expressed in mg/L, whereas those of trace elements, TEs, in μg/L).

Parameter	S5	S6	S7	S8	S9	Legal limit *
pH	8.01	7.91	7.96	8.11	7.32	
EC (S/m)	0.1492	0.1432	0.0842	0.1414	0.1492	
$N\text{-}NH_4$	0.21	0.15	0.21	0.63	5.72	0.03; 0.24
$N\text{-}NO_2$	0.076	0.027	0.030	0.049	0.040	
$N\text{-}NO_3$	1.51	1.96	1.22	1.69	2.26	0.60; 4.80
$P\text{-}PO_4$	0.062	0.052	0.150	0.100	0.520	0.05; 0.40
F^-	0.31	0.26	0.23	0.33	0.32	
Cl^-	308	300	251	103	249	
SO_4^{2-}	65.4	62.9	56.5	34.4	56.1	
Ca	99.7	99.7	92.6	97.0	106	
K	12.6	12.0	11.0	10.1	23.9	
Mg	44.2	43.0	38.4	28.2	40.2	
Na	199	188	161	70.4	150	
Al	86.7	75.2	108	60.0	70.5	
As	1.40	0.70	1.80	1.90	2.00	10.0
Ba	47.1	71.8	45.6	48.3	49.7	
Be	<0.50	<0.50	<0.50	<0.50	<0.50	
Cd	<0.50	<0.50	<0.50	<0.50	<0.50	≤0.45
Co	0.70	0.70	0.70	0.60	0.60	
Cr	1.60	0.90	0.60	0.70	1.50	
Cu	<10.0	<10.0	<10.0	<10.0	<10.0	
Fe	205	223	222	141	170	
Hg	<0.10	<0.10	<0.10	<0.10	<0.10	
Mn	60.3	110	61.5	52.6	59.5	
Ni	2.50	3.30	4.80	3.40	4.10	
Pb	<1.00	<1.00	<1.00	<1.00	<1.00	1.30
Sb	<0.20	<0.20	<0.20	<0.20	<0.20	
Se	1.04	<1.00	<1.00	<1.00	<1.00	
V	9.80	7.00	4.70	5.10	8.70	

* Limit imposed by Ministerial decree 260/10 that is enforceable of the Legislative Decree 152/06. The law states five water quality classes based on the values of dissolved oxygen, $N\text{-}NH_4$, $N\text{-}NO_3$, and P_{tot}. The values represent the limits below/above, defining the best and the worst water quality class.

Table 7 shows the concentrations of chlorophyll-a, Chl-a, phaeopigments, Phaeo, Phaeo/Chl-a, and Shannon Index. The mean levels of Chl-a and Phaeo were rather constant in all the estuary, 58.8 and 24.3 μg/L, with peaks of 95.7 and 58.0 μg/L at S7 and S2, respectively. The high primary production at S7 is due to the observed input of wastewaters in this area. It was also interesting to note a very high value of Chl-a at S2, 89.8 μg/L, revealing that the plume of anthropic pollution moves towards the outer part of the estuary. These values find confirmation from the Phaeo/Chl-a, which is lower in IE, ~0.20, and takes higher values up to 2.54 in OE.

Table 7. Water concentrations of Chlorophyll-a (Chl-a), phaeopigments (Phaeo), Phaeo/Chl-a, and Shannon Index.

Station	Chl-a (μg/L)	Phaeo (μg/L)	Phaeo/Chl-a	Shannon index
S1	62.62	22.14	0.35	1.42
S2	89.76	57.96	0.65	1.66
S3	31.15	12.79	0.41	1.60
S4	46.27	11.75	0.25	1.24
S5	15.05	38.14	2.54	1.58
S6	66.35	15.23	0.23	1.18
S7	95.70	23.93	0.25	1.08
S8	63.15	12.50	0.20	1.17

The screening of the total phytoplankton biomass revealed the presence of two main functional groups, cryptophytes, 37.6%, and diatoms, 33.8%. Whereas diatoms appeared to be homogenously distributed throughout the estuary, cryptophytes tended to increase from OE to IE, 29.5–45.8%. This seems related to the observed water salinity differences between IE and OE, i.e., lower loads of chlorides 103 vs. 308 mg/L. The association between cryptophytes and salinity is also observed in the literature [56,57]. The mean value of the Shannon index was 1.37, Table 7, with greater functional phytoplankton diversity in OE respect to IE, 1.48 vs. 1.25.

4. Conclusions

The overall data reveals how the studied estuary presents two well-defined areas, an outer and inner part with different degrees of pollution. It is clearly evident how the anthropic pressure is higher in the inner part of the estuary with higher accumulation of TOC and TN. The spatial variations of TOC, TN, and C/N evidence that organic matter from anthropogenic activities has a more significant influence than from natural processes. The high TN concentrations correspond well with high TOC in fluvial sediments, which serve as the main pathway for urban runoff, sewage, and industrial wastewater discharge. There is also a high correlation between chemical data and phytoplankton biomass with wastewaters discharges and with morphological estuary characteristics, as low depth and low hydrodynamic energy. Calcareous meiofaunal assemblages and morphoscopic analysis appear to be influenced by continental erosion, which also includes microfossils and quartz grains of the Pleistocene paleodune of Gromola. The data indicate that the Sele estuary is affected by significant geomorphological alteration due to erosion processes as well as by a conspicuous anthropic influence threatening the overall ecosystem.

Author Contributions: M.A., conceptualization, writing, methodology, roles/writing—original draft; F.B., investigation, format analysis; G.A., data curation; formal analysis; D.B., data curation; formal analysis; C.D., investigation; software, writing; C.S., data curation, formal analysis, validation; L.F., conceptualization, methodology, roles/writing—original draft; O.M., investigation, format analysis; M.T. (Maria Toscanesi), data curation, formal analysis, validation; A.G., data curation, formal analysis, validation; M.T. (Marco Trifuoggi), conceptualization, methodology, investigation. All authors have read and agreed to the published version of the manuscript.

Funding: This research received no external funding.

Acknowledgments: The authors wish to thank the kind collaboration of the Natural Reserve Authority 'Sele-Tanagro', the association ARS-Sele-Tanagro, and Fernando Guerra for providing and skippering the boat.

Conflicts of Interest: The authors declare no conflict of interest.

References

1. Bruner de Miranda, L.; Andutta, F.P.; Kjerfve, B.; Castro Filho, B.M. *Fundamentals of Estuarine Physical Oceanography*; Springer: Singapore, 2017; pp. 480.
2. Ferronato, A.; Lionello, M.; Ostoich, M.; Sanavio, G. Elementi di identificazione delle acque di transizione. ARPAV, CTN-AIM (ANPA-ARPAT) 2000, pp. 65.
3. Elliott, M.; Day, J.W.; Ramachandran, R.; Wolanski, E. Chapter 1. A Synthesis: What is the Future for Coasts, Estuaries, Deltas and Other Transitional Habitats in 2050 and Beyond? In *Coasts and Estuaries, The Future*; Wolanski, E., Day, J.W., Elliott, M., Ramachandran, R., Eds.; Elsevier: Amsterdam, The Netherland, 2019; pp. 1–28.
4. Bramanti, A. Lagune E Stagni Costieri: Due Ambienti A Confronto. In *Le Lagune Costiere: Ricerca E Gestione*; Carrada, G.C., Cicogna, F., Fresi, E., Eds.; CLEM Pubblicatio: Massa Lubrense, Napoli, Italy, 1988; pp. 9–33.
5. Valentini, A. Gli ambienti salmastri. Atti di Ostiazzurra. WWF/EC, 2000 Seminar 1: "Water and Agriculture" **1997**, 35–39.
6. Jones, N.V.; Elliott, M. The Humber Estuary and adjoining Yorkshire & Lincolnshire coasts. Coastal zone topics: Process, ecology & management; Estuarine & Coastal Sciences Association, 2000; pp. 180.
7. UNEP/MAP. State of the Mediterranean Marine and Coastal Environment. UNEP/MAP–Barcelona Convention, Athens, 2012.
8. Wolanski, E.; Day, J.W.; Elliott, M.; Ramachandran, R. *Coasts and Estuaries: The Future*; Elsevier: Amsterdam, The Netherland, 2019; pp. 687.
9. Di Paola, G.; Aucelli, P.P.C.; Benassai, G.; Rodríguez, G. Coastal vulnerability to wave storms of Sele littoral plain (southern Italy). *Nat. Hazards* **2014**, *71*, 1795–1819.
10. Cocco, E.; De Magistris, M.A.; De Pippo, T.; Efaicchio, M.T.; Valente, A. Coastal Dynamics Along the Shores of Campania and Lucania (Southern Italy). Proceedings of the Sixth Symposium on Costal and Ocean Management, Charleston, SC, USA, 1989; Volume 3, pp. 2794–2807.
11. D'Acunzi, G.; De Pippo, T.; Donadio, C.; Peduto, F.; Santoro, U.; Sessa, F.; Terlizzi, F.; Turturiello, M.D. Studio dell'evoluzione della linea di costa della piana del Sele (Campania) mediante l'uso della cartografia numerica. *Stud. Costieri* **2008**, *14*, 55–67.
12. Freeman, M.C.; Pringle, C.M.; Jackson, C.R. Hydrologic connectivity and the contribution of stream headwaters to ecological integrity at regional scales. *J. Am. Water Res. Assoc.* **2007**, *43*, 5–14.
13. Magdaleno, F.; Donadio, C.**;** Kondolf, G.M. 30 year response to damming of a Mediterranean river in California, USA. *Phys. Geogr.* **2018**, *39*, 197–215.
14. Pappone, G.; Alberico, I.; Amato, V.; Aucelli, P.P.C.; Di Paola, G. Recent evolution and the present-day conditions of the Campanian Coastal plains (South Italy): The case history of the Sele River Coastal plain. *WIT Trans. Ecol. Environ.* **2011**, *149*, 15–27, doi:10.2495/CP110021.
15. Barra, D.; Calderoni, G.; Cinque, A.; De Vita, P.; Rosskopf, C.M.; Russo Ermolli, E. New data on the evolution of the Sele River coastal plain (Southern Italy) during the Holocene. *Il Quat. Italian J. Quat. Sci.* **1998**, *11*, 287–299.
16. Cinque, A. Guida alle escursioni geomorfologiche (Penisola Sorrentina, Capri, Piana del Sele e Monti Picentini). Riunione annuale del Gruppo Nazionale Geografia Fisica e Geomorfologia, Amalfi 1986. Pubbl. n. 33 del Dipartimento di Scienze della Terra, Università Federico II di Napoli, 1986.
17. Brancaccio, L.; Cinque, A.; D'Angelo, G.; Russo, F.; Santangelo, N.; Sgrosso, I. Evoluzione tettonica e geomorfologica della Piana del Sele (Campania, Appennino meridionale). *Geogr. Fis. Dinam. Quat.* **1987**, *10*, 47e55.
18. Barra, D.; Calderoni, G.; Cipriani, M.; De La Genieré, J.; Fiorillo, L.; Greco, G.; Mariotti Lippi, M.; Mori Secci, M.; Pescatore, T.; Russo, B.; et al. Depositional history and paleogeographic reconstruction of Sele coastal plain during Magna Grecia settlement of Hera Argiva (Southern Italy). *Geol. Romana* **1999**, *35*, 151–166.
19. Cinque, A.; Romano, P.; Budillon, F.; D'Argenio, B. Note illustrative della Carta Geologica d'Italia alla scala 1:50.000. Foglio 486, Foce Sele. ISPRA, Servizio Geologico d'Italia, 2009, pp. 144.
20. Arienzo, M.; Albanese, S.; Lima, A.; Cannatelli, C.; Aliberti, F.; Cicotti, F.; Qi, S.; De Vivo, B. Assessment of the concentrations of polycyclic aromatic hydrocarbons and organochlorine pesticides in soils from the Sarno River basin, Italy, and ecotoxicological survey by Daphnia magna. *Environ. Monit. Assess.* **2015**, *187*, 4272–4275.

21. Albanese, S.; Iavazzo, P.; Adamo, P.; Lima, A.; De Vivo, B. Assessment of the environmental conditions of the Sarno river basin (south Italy): A stream sediment approach. *Environ. Geochem. Health* **2013**, *35*, 283–297.
22. Angelucci, A.; Palmerini, V. Studio sedimentologico delle sabbie rosse di Piverno (Lazio sud-occidentale). *Geol. Romana* **1964**, *3*, 203–226.
23. Bui, E.N.; Mazullo, J.; Wilding, L.P. Using quartz grain size and shape analysis to distinguish between aeolian and fluvial deposits in the Dallol Bosso of Niger (West Africa). *Earth Surf. Process. Landf.* **1990**, *14*, 157–166.
24. Belloni, S. Una tabella universale per eseguire granulometrie col metodo della sedimentazione unica o col metodo del densimetro di Casagrande modificato. *Geol. Tec*. **1969**, *16*, 1281–1289.
25. Folk, R.L.; Ward, W.C. Brazos River bar: A study in the significance of grain size parameters. *J. Sediment. Petrol* **1957**, *27*, 3–26.
26. Blott, S.J.; Pye, K. GRADISTAT: A particle size distribution and statistics package for the analysis of unconsolidated sediments. *Earth Surf. Process. Landf.* **2001**, *26*, 1237–1248.
27. Graham, D.; Midgley, N.G. Graphical representation of particle shape using triangular diagrams: An excel spreadsheet method. *Earth Surf. Process. Landf.* **2000**, *25*, 1473–1477.
28. Cicchella, D.; De Vivo, B.; Lima, A.; Albanese, S.; Mc Gill, R.A.R.; Parrish, R.R. Heavy metal pollution and Pb isotopes in urban soils of Napoli, Italy. *Geochem. Explor. Environ. Anal.* **2008**, *8*, 19–29.
29. Arienzo, M.; Donadio, C.; Mangoni, O.; Bolinesi, F.; Stanislao, C.; Trifuoggi, M.; Toscanesi, M.; Di Natale, G.; Ferrara, L. Characterization and source apportionment of polycyclic aromatic hydrocarbons (PAHs) in the sediments of gulf of Pozzuoli (Campania, Italy). *Mar. Pollut. Bull.* **2017**, *124*, 480–487.
30. Hansen, H.P.; Grasshoff, K. Automated Chemical Analysis. In *Methods of Seawater Analysis*, 3rd ed.; Grasshoff, K., Kremlin, K., Ehrhardt, M.; WILEY-VCH: Weinheim, Germany, 1999.
31. APAT CNR-IRSA Metodi analitici per le acque. Manuali e Linee Guida 29/2003 2003.
32. UNI EN ISO Qualità Dell'acqua. *Applicazione Della Spettrometria Di Massa Al Plasma Accoppiato Induttivamente (ICP-MS)—Parte 2: Determinazione Di Elementi Selezionati, Compresi Gli Isotopi Dell'uranio*; UNICHIM: Milano, Italy, 2016.
33. Vidussi, F.; Claustre, H.; Bustillos-Guzman, J.; Cailliau, C.; Marty, J.C. Determination of chlorophylls and carotenoids of marine phytoplankton: Separation of chlorophyll a from divinyl-chlorophyll a and zeaxanthin from lutein. *J. Plank. Res.* **1996**, *18*, 2377–2382.
34. Mangoni, O.; Aiello, G.; Balbi, S.; Barra, D.; Bolinesi, F.; Donadio, C.; Ferrara, L.; Guida, M.; Parisi, R.; Pennetta, M.; et al. A multidisciplinary approach for the characterization of the coastal marine ecosystems of Monte Di Procida (Campania, Italy). *Mar. Pollut. Bull.* **2016**, *112*, 443–451.
35. Jeffrey, S.W. Algal Pigment Systems. In *Primary Productivity in the Sea*; Falkowski, P.G., Ed.; Plenum: New York, NY, USA, 1980; pp. 33–58.
36. Herbland, A. The Deep Phaeopigments Maximum in the Ocean: Reality or Illusion? In *Toward a Theory on Biological-Physical Interactions in the World Ocean*; Rothschild, B., Ed.; Kluwer Academic: Amsterdam, The Netherland, 1988; pp. 157–172.
37. Taguchi, S.; Laws, E.A.; Bidigare, E.R. Temporal variability in chlorophyll *a* and phaeopigment concentrations during incubations in the absence of grazers. *Mar. Ecol. Prog. Ser.* **1993**, *101*, 45–53.
38. Mackey, M.D.; Mackey, D.J.; Higgins, H.W.; Wright, S.W. CHEMTAX—A program for estimating class abundances from chemical markers: Application to HPLC measurements of phytoplankton. *Mar. Ecol. Prog. Ser.* **1996**, *144*, 265–283.
39. Mangoni, O.; Modigh, M.; Mozetic, P.; Bergamasco, A.; Rivaro, P.; Saggiomo, V. Structure and photosynthetic properties of phytoplankton assemblages in a highly dynamic system, the Northern Adriatic Sea. *Est. Coast. Shelf Sci.* **2008**, *77*, 633–644.
40. Cinque, A.; Romano, P.; Boudillon, F.; D'Argenio, B. Explanatory Notes to Geological Map of Italy, scale 1:50,000-Sheet 486 Foce del Sele. *ISPRA Servizio Geologico d'Italia* 2009.
41. Li, L.; Gallagher, S.; Finlayson, B. Foraminiferal response to Holocene environmental changes of a tidal estuary in Victoria, southeastern Australia. *Mar. Micropaleontol.* **2000**, *38*, 229–246.
42. Ghosh, A.; Saha, S.; Saraswati, P.K.; Banerjee, S.; Burley, S. Intertidal foraminifera in the macro-tidal estuaries of the Gulf of Cambay:Implications for interpreting sea-level change in palaeo-estuaries. *Mar. Petr. Geol.* **2009**, *26*, 1592–1599.
43. Meisch, C. *Freshwater Ostracoda of Western and Central Europe*; Spektrum Akademischer Verlag: Berlin/Heidelberg, Germany, 2000; p. 522.

44. Avramidisa, P.; Nikolaoua, K.; Bekiarib, V. Total Organic Carbon and Total Nitrogen in Sediments and Soils: A Comparison of the Wet Oxidation-Titration Method with the Combustion-Infrared Method. *Agric. Agric. Sci. Proc.* **2015**, *4*, 425–430.
45. Carroll, M.L.; Cochrane, S.; Fieler, R.; Velvin, R.; White, P. Organic enrichment of sediments from salmon farming in Norway: Environmental factors, management practices, and monitoring techniques. *Aquaculture* **2003**, *226*, 165–180.
46. Schaanning, M.T. *Distribution of Sediment Properties in Coastal Areas Adjacent to Fish Farms and Environmental Evaluation of Five Locations Surveyed in October 1993*; Report No. O-93205, O-93062; Norwegian Institute for Water Research (NIVA): Oslo, Norway, 1994.
47. Nixon, S.W. Coastal marine eutrophication: A definition, social causes, and future concerns. *Ophelia* **1995**, *41*, 199–219.
48. Graham, M.C.; Eaves, M.A.; Farmer, J.G.; Dobson, J.; Fallick, A.E. A study of carbon and nitrogen stable isotope and elemental ratios as potential indicators of source and fate of organic matter in sediments of the Forth Estuary, Scotland. *Estuar. Coast. Shelf Sci.* **2001**, *52*, 375–380.
49. Lamb, A.L.; Wilson, G.P.; Leng, M.J. A review of coastal palaeoclimate and relative sea-level reconstructions using d13C and C/N ratios in organic material. *Earth Sci. Rev.* **2006**, *75*, 29–57.
50. Ministero dell'Ambiente e della Tutela del Territorio. Decreto 6 Novembre 2003, n. 367. Regolamento concernente la fissazione di standard di qualità nell'ambiente acquatico per le sostanze pericolose, ai sensi dell'articolo 3, comma 4, del decreto legislativo 11 maggio 1999, n. 152. Gazzetta Ufficiale della Repubblica Italiana n. 5 dell'8 gennaio 2004.
51. Wilson, S.C.; Lockwood, P.V.; Ashley, P.M.; Tighe, M. The chemistry and behaviour of antimony in the soil environment with comparisons to arsenic: A critical review. *Environ. Pollut.* **2010**, *158*, 1169–1181.
52. Dubinin, A.V. Geochemistry of rare earth elements in the ocean. *Lithol. Miner. Resour.* **2004**, *39*, 289–307.
53. Liu, X.J.; Ge, C.D. Spatial and temporal variations of sedimented organic matter in Xiaohai Lagoon, Hainan Island. *Acta Oceanol. Sin.* **2012**, *31*, 74–87.
54. Lebart, L.; Morineau, A.; Warwick, K.M. *Multivariate Descriptive Statistical Analysis*; John Wiley & Sons: New York, NY, USA, 1984.
55. Vaisanen, U.; Misund, A.; Chekushin, V. Ecogeochemical investigation: Stream water quality as an indicator of pollution in the border areas of Finland, Norway and Russia. *Water Air Soil Pollut.* **1998**, *104*, 205–219.
56. Mendes, C.R.B.; Tavano, V.M.; de Souza, M.S.; Garcia, C.A.E. Shifts in the dominance between diatoms and cryptophytes during three late summers in the Bransfield Strait (Antarctic Peninsula). *Polar Biol.* **2013**, *36*, 537–547.
57. Johnson, A.N. Effects of Salinity and Temperature on Phytoplankton Community of San Francisco Estuary. Doctoral Thesis, San Francisco State University, San Francisco, CA, USA, 2015; p. 72.